ELSEVIER

Superlattices and Microstructures 36 (2004) 95–105

Superlattices
and Microstructures

www.elsevier.com/locate/superlattices

Patterned growth of aligned ZnO nanowire arrays on sapphire and GaN layers

H.J. Fan[a,*], F. Fleischer[a], W. Lee[a], K. Nielsch[a], R. Scholz[a], M. Zacharias[a], U. Gösele[a], A. Dadgar[b], A. Krost[b]

[a] *Max Planck Institute of Microstructure Physics, Weinberg 2, 06120 Halle, Germany*
[b] *Institute of Experimental Physics, Otto-von-Guericke University, 39016 Magdeburg, Germany*

Available online 15 September 2004

Abstract

Patterned growth of vertically aligned ZnO nanowire arrays on the micrometer and nanometer scale on sapphire and GaN epilayers is reported. In order to control the position and distribution density of the ZnO nanowires, Au seeding nanodots are defined, as regular arrays, with the assistance of deposition shadow masks. Electron micrographs reveal that the wires are single crystals having wire axes along the hexagonal *c*-axes. The epitaxial growth of ZnO nanowires on sapphire and GaN films on Si substrates was further verified by cross sectional electron microscopy investigations. Compared to the sapphire case, the perfect epitaxial growth on a GaN film on a Si substrate is believed to be more suitable for potential electronic device applications of ZnO nanowire arrays.

Keywords: Zinc oxide; Semiconductor nanowire; Nanopatterning; Epitaxial growth

1. Introduction

ZnO is a direct wide bandgap (3.37 eV) semiconductor with a large excitation binding energy (60 meV). ZnO-based one-dimensional (1D) nanoscale materials, as important functional oxide nanostructures, have received increasing attention over the past

* Corresponding author. Tel.: +49 345 558 2760; fax: +49 345 551 1223.
E-mail address: hjfan@mpi-halle.de (H.J. Fan).

0749-6036/$ - see front matter © 2004 Published by Elsevier Ltd
doi:10.1016/j.spmi.2004.08.028

Table 1
The crystal structure and lattice constants of ZnO, GaN, and sapphire

Crystal structure	GaN	ZnO	Sapphire
	Wurtzite	Wurtzite	Hexagonal
Lattice constants (nm)	$a = 3.189$ $c = 5.185$	$a = 3.249$ $c = 5.207$	$a = 4.754$ $c = 12.99$
Epitaxial relationship and lattice constant misfit	ZnO(0001)[11$\bar{2}$0] ∥ GaN(0001)[11$\bar{2}$0] misfit: 1.9%		
	ZnO(0001)[11$\bar{2}$0] ∥ Al_2O_3(11$\bar{2}$0)[0001] misfit: 0.08%		

few years due to their potential applications in optoelectronic switches, high-efficiency photonic devices, near-UV lasers, and assembling complex three-dimensional nanoscale systems [1–6]. These device applications might be reinforced if the position, orientation, composition, and shape of the nanostructures can be controlled to a high degree of precision. For example, the field emission properties will be greatly improved (lower emission threshold and higher current density) if the 1D nanostructures are perfectly aligned perpendicularly to the substrates. It has been also shown that the light-emitting properties of ZnO are dependent on the alignment of the nanostructures. Therefore, the controlled growth of well-ordered ZnO 1D nanostructures is crucial and a number of reports have been given on the successful realization of highly ordered 1D ZnO nanostructures (wires, tubes, etc.) using various methods such as vapor transport and deposition [2], metal–organic vapor phase epitaxy (MOVPE) [7], the porous alumina template method [8].

The nanowire growth method employed in this work, known as the vapor–liquid–solid (VLS) technique, requires the aid of catalyzing metal particles, which are of Au in our case. It is therefore crucial to be able to accurately control the position of the seed particles during growth. More recently, some positioning methods have been employed to pattern the seeding particles, for example, deposition of Au through a nanochannel alumina template [9], atomic force microscope (AFM) manipulation of the seeding particles [10], electron beam lithography [11], and self-assembly nanosphere lithography [12]. The subsequent fabrication, particularly in the vapor phase, of aligned ZnO nanowires requires epitaxial growth on the substrates. While sapphire has been commonly used as a substrate for the epitaxial growth of ZnO nanowires, GaN is potentially an even better suited substrate as the latter has nearly the same lattice constants as ZnO (see Table 1). More importantly, due to the semiconducting nature of doped GaN, it looks promising to create n-ZnO/p-GaN nanostructured heterojunctions within the wires for electric device applications. More recently, Park and Yi [13] reported the MOVPE synthesis of ZnO nanowire arrays on GaN/sapphire layers and investigated the electroluminescence from the n-ZnO/p-GaN nanowire heterojunctions.

In this contribution, we report the patterned growth of ZnO nanowires on both (11$\bar{2}$0)-oriented sapphire substrates and (0001)-oriented GaN epilayers using the vapor deposition method based on the VLS mechanism. In order to control the distribution density and

position of the nanowires, the Au seeding particles were patterned by using shadow masks during the deposition process. In this work, the masks used here are transmission electron microscopy (TEM) grids and membranes containing an array of nanoholes. The crystalline properties of the nanowires and the wire/substrate interfaces were investigated by TEM.

2. Experiments

The n-doped GaN epilayers, 500 nm in thickness, were grown by MOVPE on Si(111) [14]. Before the deposition of the GaN film, a ∼25 nm thick AlN buffer layers was grown to avoid melt-back etching. Prior to the nanowire growth experiments, the GaN/AlN/Si substrates were coated with Au by plasma sputtering. In order to create Au patterns, two kinds of shadow masks were used. The first is a 2000-square-mesh TEM grid. The second kind are membranes containing polydomain hexagonal array of nanoholes, which were electrochemically fabricated from a nanoporous alumina membrane. The nanohole size is ∼150 nm and the inter-hole distance is around 500 nm. After removing the shadow masks, a polydomain array of Au nanodots was obtained.

Growth of ZnO nanowires is performed inside a horizontal quartz tube (inner diameter: 5 cm; heating zone: 18 cm). An alumina boat loaded with a mixture of ZnO + C (1:1) powder was placed at the center of the tube. The Au-coated substrates were located over the source boat with the Au coating facing downward. The chamber was evacuated to a background pressure of $\sim 10^{-2}$ Pa and this was followed by an Ar gas flush. Upon the equilibrium of a gas flow at 25 sccm, the tube was heated by a resistance furnace to and kept at 850 °C for 30 min. During the whole process, the tube pressure was maintained at 2×10^4 Pa by means of an electronic needle valve and pumping. The structure of the synthesized products was characterized using a scanning electron microscope (SEM, JEOL JSM-6300F), X-ray diffraction (XRD), TEM (Philips CM20T), and high-resolution TEM (HRTEM, JEOL JEM-4010).

3. Results and discussion

Figs. 1 and 2 show the results of patterned growth of ZnO nanowire arrays on *a*-plane sapphire and GaN layers, respectively. For these experiments, TEM grids were used as the deposition mask to create an Au square matrix. It can be clearly seen that a high density ($\sim 10^7$ mm^{-3}) of vertically oriented ZnO nanowires was achieved only in the Au-coated squares, while no wires were grown in the inter-square area. This is a strong indication of the catalyst-assisted growth process. The dispersion of the nanowire arrays is fairly uniform throughout the whole TEM grid-covered area. In fact, when the Au film is deposited on the whole substrate surface, the growth results in a film of nanowire arrays covering the entire surface. Hence, the nanowire fabrication can be realized on a large scale. The nanowires have diameters of 30–80 nm and lengths of around 5 μm, depending on the growth time (30 min herein), the local vapor pressure of the reactants (governed by the sampling geometry) and the Au particle size (determined by the Au film thickness). In Figs. 1 and 2, the Au film thickness is ∼2 nm. Generally, prolonged growth and larger Au film thickness result in nanowires with larger diameter and length. The orientation

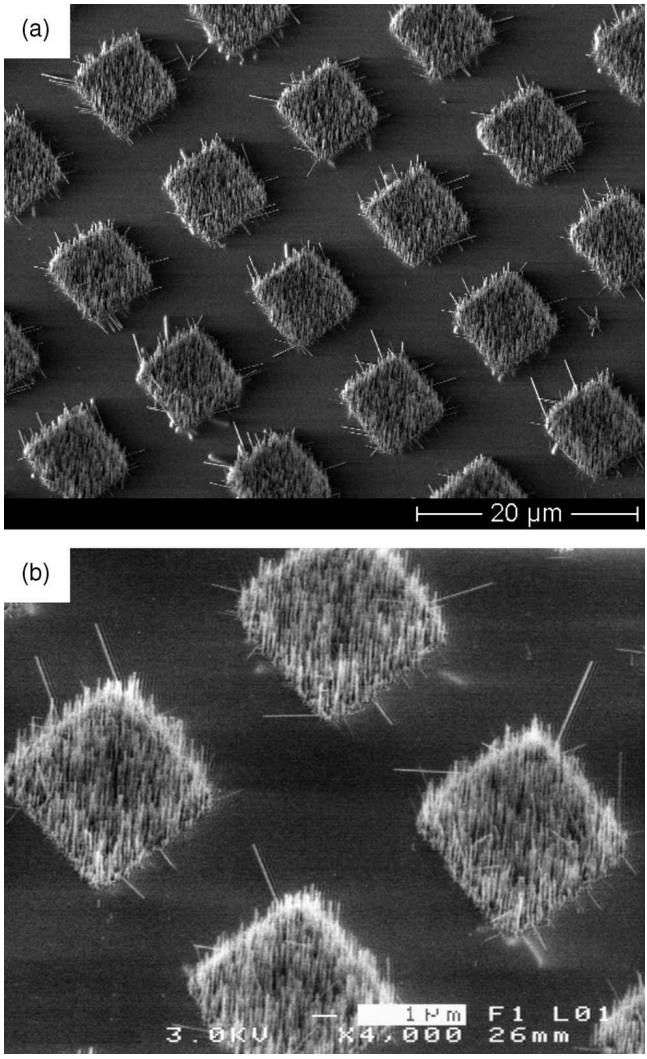

Fig. 1. ZnO nanowires grown on patterned *a*-plane sapphire. (a) A low-magnification image showing the nanowires in squares; (b) a high-magnification view of the nanowire arrays. Prior to the nanowire growth, the Au pattern was created using the shadow mask of a TEM grid during the deposition process.

of the nanowire arrays relative to the GaN layer has been studied by means of XRD. It was found that the results prior to and after the growth of nanowires show no significant difference. This is not surprising since, due to the crystal structure being the same and the lattice constants being similar (see Table 1), the (0001)-oriented GaN and ZnO have almost overlapping XRD profiles. However, the fact that no additional peaks other than the (0002) and (0004) peaks appear in the XRD spectra strongly supports the good alignment of the ZnO nanowires along the hexagonal *c*-direction.

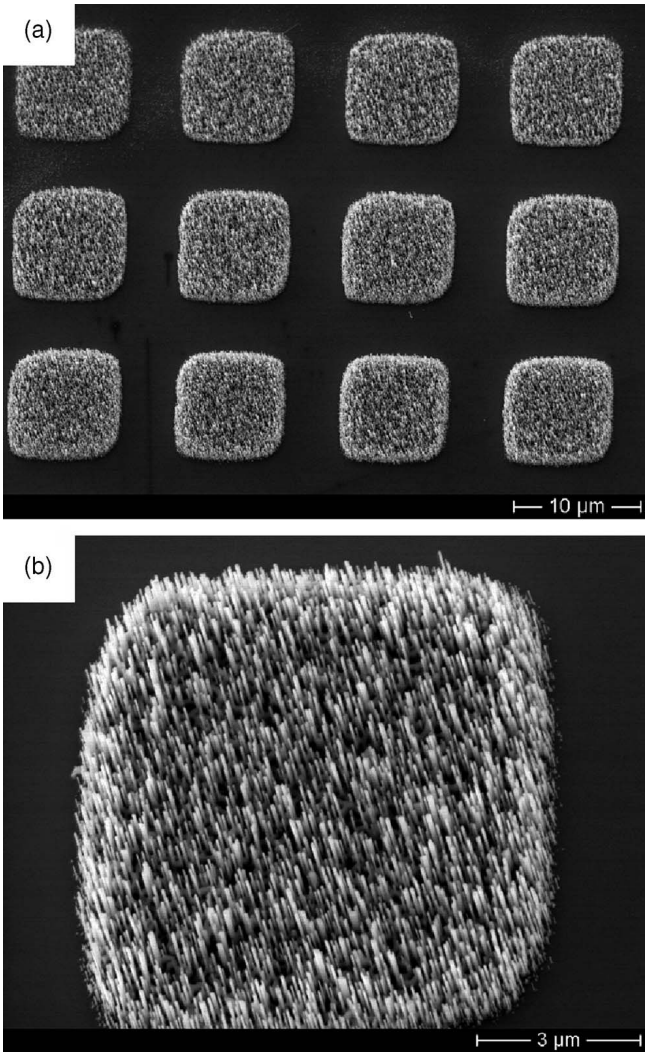

Fig. 2. ZnO nanowires grown on patterned GaN/AlN/Si substrate. (a) A low-magnification image showing the nanowires in squares; (b) a high-magnification image showing the nanowires in one square. Prior to the nanowire growth, the Au pattern was created using the shadow mask of a TEM grid during the deposition process.

It is noteworthy that the general morphology of the nanowire arrays on sapphire (Fig. 1) differs slightly from that on GaN layers (Fig. 2). As is evident from Fig. 1, although most of the nanowires stand vertical to the sapphire surface plane, some wires are readily visible which are nearly lying in the surface plane. Considering that the inclination angles (the angle between the wire axis and the sapphire surface plane) are around 30° and that the relative angles between the inclined wires, in a top view, are 60°, the presence of the inclined wires is probably due to epitaxial growth from the vicinal $\{11\bar{2}0\}$ planes in the

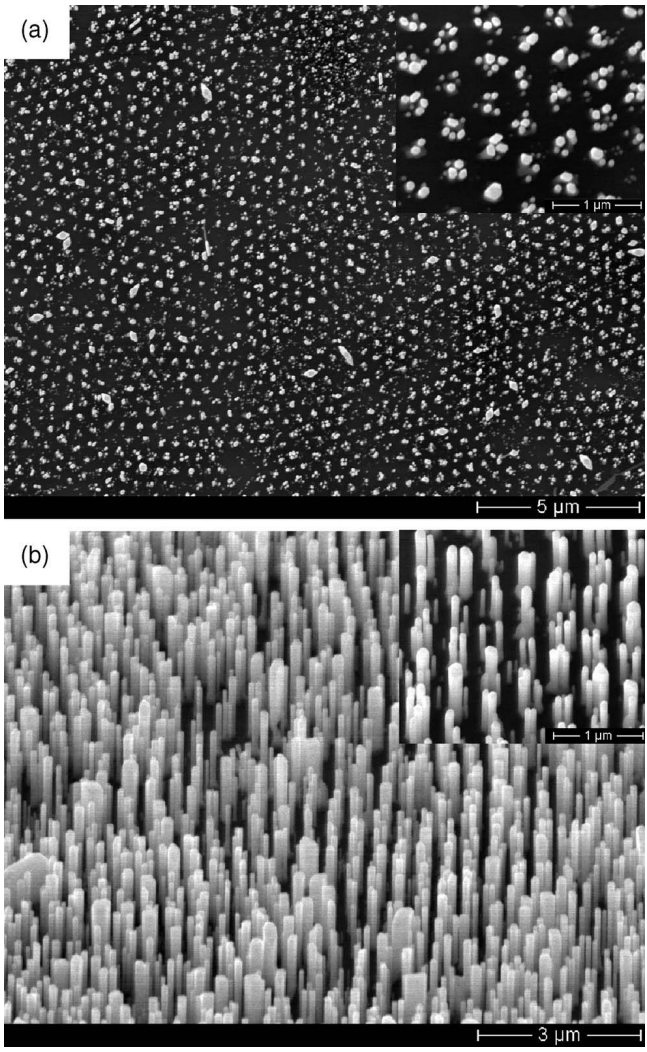

Fig. 3. ZnO nanowire arrays grown on GaN/AlN/Si substrate. (a) The top view; (b) a perspective view. The insets show a portion of the sample surface at high magnifications. Prior to the nanowire growth, the polydomain Au nanodot array was created by sputtering Au through a membrane mask of Au nanotubes arrays followed by removal of the mask.

a-plane sapphire. In contrast, when GaN epilayers are used as substrates, all the nanowires grown are uniformly oriented without any inclined wires at all (see Fig. 2). This implies that the GaN layers are much more advantageous compared with sapphire as substrates for such highly ordered ZnO nanowires.

While the above results demonstrate patterned growth of nanowire arrays on a micrometer scale, further scaling down of the patterning to the nanometer range has been

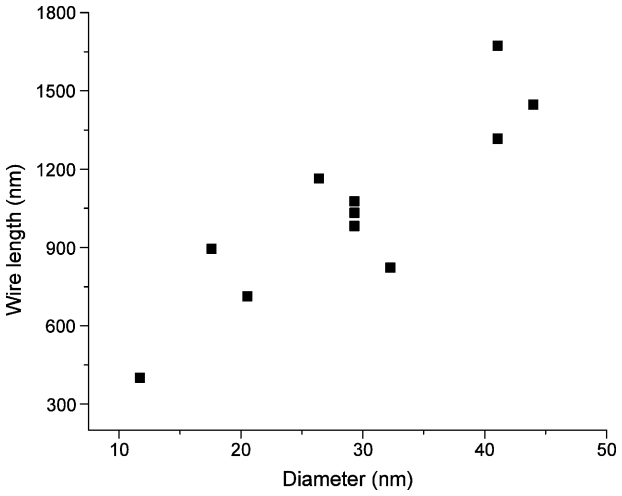

Fig. 4. The length versus diameter relationship of ZnO nanowires grown on the GaN epilayers.

attempted. To implement this, a polydomain array of Au nanodots on the GaN substrate was made by sputtering Au through a shadow mask which was electrochemically fabricated from a porous alumina membrane. Fig. 3 shows the result of nanowire growth on the GaN layer. The top view of the wire arrays (see Fig. 3(a)) reveals that the ZnO nanowires grow at the position of the Au particles, and the original polydomain pattern was reasonably retained. We believe that our patterned growth is independent of the method used for producing the Au arrangements. Such experimental flexibility will be of benefit for future device applications of the ZnO nanowire arrays.

It is noteworthy that, as seen in Fig. 3(b), generally three or four nanowires grow from one Au dot area, and the thick wires are longer than the thin ones. This might be explained by thermodynamics. At the high growth temperature, a molten Au particle (original size $\sim$150 nm) becomes thermodynamically unstable, and thus moves to the substrate surface and splits into several smaller nanodots. The small Au nanodots are more favorable than large ones when a VLS growth process under specific conditions is involved. Also, the trend that large-sized wires grow faster than smaller ones (see Fig. 4) can be qualitatively explained in terms of the Gibbs–Thomson effect [15], i.e., increasing Zn vapor pressure and thereby decreasing supersaturation as the nanowire diameter becomes smaller.

In order to confirm the single-crystalline quality and orientation of the nanowires, TEM investigations were conducted. Fig. 5(a) shows a low-magnification TEM image of ZnO nanowires scratched from the sapphire surface. Consistent with SEM observations, the wires have the shape of rods and diameters of 20–50 nm. It is noted that the ripple-like contrast is due to stress. The HRTEM image in Fig. 5(b) clearly reveals a well-resolved lattice with the measured inter-plane spacing of $\approx$0.52 nm. Moreover, the nanowire growth direction, determined from both the HRTEM image and the ED pattern in Fig. 5(a), is along [0001], which is the fastest growth direction for ZnO crystals. Taken together, our ZnO nanowires are single-crystalline wurtzite structured and *c*-axis elongated. It should

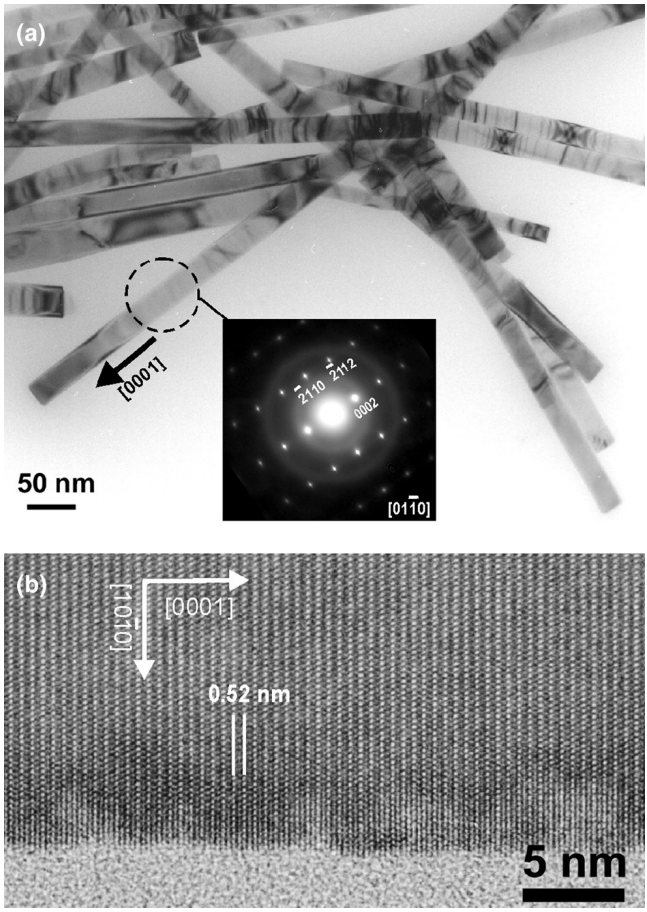

Fig. 5. (a) A TEM image of the ZnO nanowires. The ED pattern in the inset indicates that the wire axis direction is [0001]. (b) An HRTEM lattice image at the edge of a ZnO nanowire, confirming that the wire is single crystal with wurtzite structure.

be pointed out that the presence of Au alloy droplets at the tips of the nanowires, which is characteristic of VLS growth, was not observed in our TEM investigations. A possible reason is that the Au droplet was unstable on the nanowire tip and dropped down. After the Au droplet was gone, the nanowire tip became smooth again by the self-arrangement of the surface atoms. A detailed compositional analysis by e.g., X-ray photoemission spectroscopy, will be necessary in the future.

The epitaxial growth was confirmed on the basis of cross sectional TEM investigations at the nanowire/substrate interfaces. Fig. 6 shows the ED patterns recorded at the ZnO/Al_2O_3 interface region. Indexing the ED patterns reveals that the [11$\bar{2}$0] direction of ZnO is parallel to the [0001] direction of the *a*-plane Al_2O_3 substrate, consistently with the result reported by Wu et al. [2]. As for the GaN, a direct image of the lattice

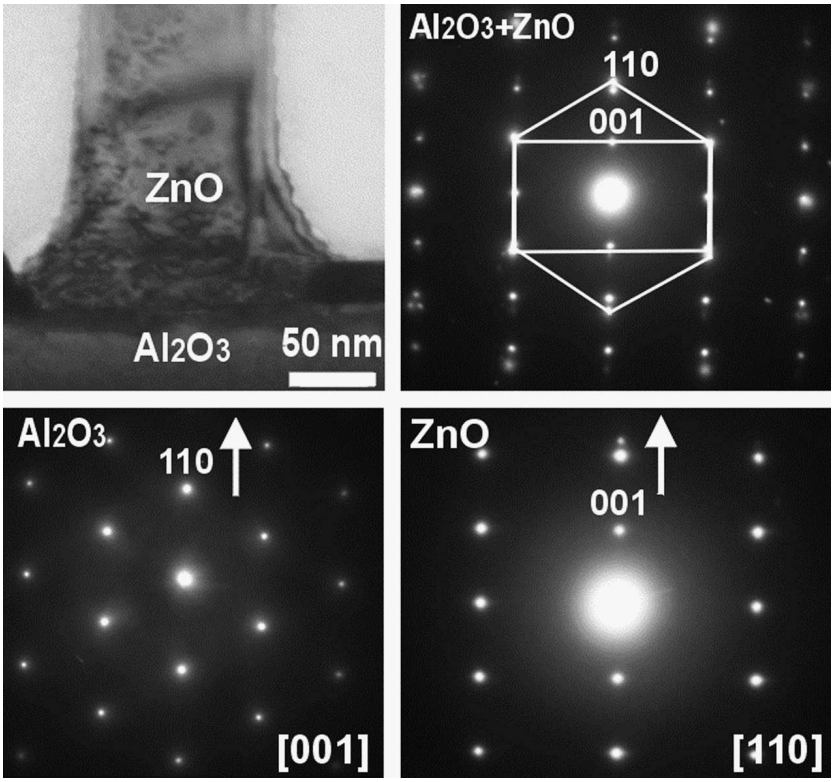

Fig. 6. A cross sectional TEM image recorded at the ZnO/sapphire interface and the ED patterns corresponding to different regions in the TEM image. The epitaxial relationship is ZnO(0001)[11$\bar{2}$0] ∥ Al_2O_3(11$\bar{2}$0)[0001].

structure at the ZnO/GaN interface is illustrated, in Fig. 7(a). A semicoherent interface along the [10$\bar{1}$0] direction between the bottom of the ZnO nanowire and the GaN layer is observable, and the (0001) planes are perfectly parallel. Fig. 7(b) is the selected area ED pattern at the interface. The pattern can be indexed as [11$\bar{2}$0] zone axis hexagonal wurtzite ZnO and GaN, confirming the good lattice match seen in the (11$\bar{2}$0) directions. Taking these findings together, it is verified that the ZnO nanowires grow epitaxially on the GaN epilayer with ZnO(0001)[11$\bar{2}$0] ∥ GaN(0001)[11$\bar{2}$0]. This result supports the assertion that the (0001)-oriented GaN-on-Si layers are ideally suited substrates for the fabrication of highly ordered ZnO nanowire arrays.

4. Conclusions

In summary, the patterned growth of vertically aligned single-crystalline ZnO nanowire arrays on (11$\bar{2}$0)-oriented sapphire substrates and (0001)-oriented GaN epilayers has been demonstrated. We have shown that the ZnO nanowires are adjustable in their position and distribution density when the seeding Au particles are predefined into regular arrays.

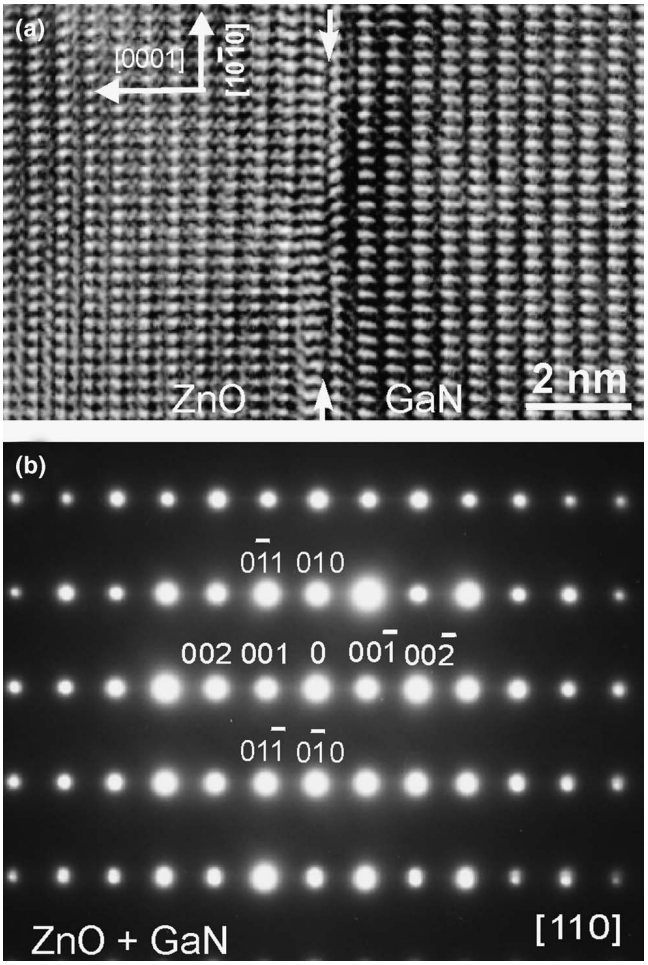

Fig. 7. A cross sectional HRTEM lattice image recorded at the ZnO/GaN interface and the corresponding ED pattern, confirming the epitaxial growth of ZnO nanowires on the GaN epilayer.

Moreover, due to their semiconducting behavior and the similarity in lattice structure to ZnO, GaN epilayers could be a good candidate for use in the epitaxial growth, and subsequent device applications, of ZnO nanowire arrays. Our simple “bottom-up” approach could be generalized to fabricate many other 1D semiconductor nanostructure arrays on conductive layers.

Acknowledgments

The authors thank D.H. Bao for help with the XRD measurement, and Ms. Hopfer for TEM sample preparations.

References

[1] Y. Xia, P. Yang, Y. Sun, Y. Wu, B. Mayers, B. Gates, Y. Yin, F. Kim, H. Yan, Adv. Mater. 15 (2003) 353.
[2] Y. Wu, H. Kind, E. Weber, R. Russo, P. Yang, Science 292 (2001) 1897.
[3] H. Kind, H. Yan, M. Law, B. Messer, P. Yang, Adv. Mater. 14 (2002) 158.
[4] M.H. Huang, Y. Wu, H. Feick, G. Tran, E. Weber, P. Yang, Adv. Mater. 13 (2002) 113.
[5] M.S. Arnod, P. Avouris, Z.W. Pan, Z.L. Wang, J. Phys. Chem. B 107 (2003) 659.
[6] Y.W. Zhu, H.Z. Zahng, X.C. Sun, S.Q. Feng, J. Su, Q. Zhang, B. Xiang, R.M. Wang, D.P. Yu, Appl. Phys. Lett. 83 (2003) 144.
[7] W.I. Park, G.-C. Yi, M. Kim, S.J. Pennycook, Adv. Mater. 14 (2002) 1841.
[8] C. Liu, J.A. Zapien, Y. Yao, X. Meng, C.S. Lee, S. Fan, Y. Lifshitz, S.T. Lee, Adv. Mater. 15 (2003) 838.
[9] Z.H. Wu, X.Y. Mei, D. Kim, M. Blumin, H.E. Ruda, Appl. Phys. Lett. 81 (2002) 5177.
[10] J. Ohlsson, M.T. Bjork, M.H. Magnusson, K. Deppert, L. Samuelson, L.R. Wallenberg, Appl. Phys. Lett. 79 (2001) 3335.
[11] T. Martensson, M. Borgstrom, W. Seifert, B.J. Ohlsson, L. Samuelson, Nanotechnology 14 (2003) 1255.
[12] X. Wang, C.J. Summers, Z.L. Wang, Nano. Lett. 4 (2004) 423.
[13] W.I. Park, G.C. Yi, Adv. Mater. 16 (2004) 87.
[14] A. Dadgar, A. Strittmatter, J. Bläsing, M. Poschenrieder, O. Contreras, P. Veit, T. Riemann, F. Bertram, A. Reiher, A. Krtschil, A. Diez, T. Hempel, T. Finger, A. Kasic, M. Schubert, D. Bimberg, F.A. Ponce, J. Christen, A. Krost, Phys. Status Solidi c 0 (2003) 1583.
[15] E.I. Givargizov, J. Cryst. Growth 31 (1975) 20.